

Multi-agent Reinforcement Learning for Regional Signal control in Large-scale Grid Traffic network

Hankang Gu, Shangbo Wang

Abstract—Adaptive traffic signal control with Multi-agent Reinforcement Learning(MARL) is a very popular topic nowadays. In most existing novel methods, one agent controls single intersections and these methods focus on the cooperation between intersections. However, the non-stationary property of MARL still limits the performance of the above methods as the size of traffic networks grows. One compromised strategy is to assign one agent with a region of intersections to reduce the number of agents. There are two challenges in this strategy, one is how to partition a traffic network into small regions and the other is how to search for the optimal joint actions for a region of intersections. In this paper, we propose a novel training framework RegionLight where our region partition rule is based on the adjacency between the intersection and extended Branching Dueling Q-Network(BDQ) to Dynamic Branching Dueling Q-Network(DBDQ) to bound the growth of the size of joint action space and alleviate the bias introduced by imaginary intersections outside of the boundary of the traffic network. Our experiments on both real datasets and synthetic datasets demonstrate that our framework performs best among other novel frameworks and that our region partition rule is robust.

Index Terms—Adaptive traffic signal control, Multi-agent Reinforcement Learning, Regional control

I. INTRODUCTION

TRAFFIC congestion is becoming a significant problem that brings both financial costs and environmental damage. According to a recent study, in 2021, it costs £595 and 73 hours per driver in UK [1] while drivers in the USA spent \$ 564 each and wasted 3.4 billion hours a year in total [2]. Meanwhile, the gas emitted from transportation is now an unignorable contributor to the pollutants responsible for air pollution [3], [4]. Mitigating traffic congestion benefits economics and also human health. The traffic signal is a direct way to control traffic flows. With advanced technology and more data nowadays, it is promising to find a better way to utilise traffic signals to reduce congestion.

Classic traffic signal control(TSC) methods take rule-based signal plans such as Webster [5], [6] and MaxBand [7]. These two methods compute optimised signal plans based on traffic parameters such as traffic demand and saturation rate. However, since these two methods assume that traffic flow is uniform and intersections share the same cycle length, they hardly adapt to more complex traffic dynamics in real scenarios. Intelligent methods with a better adaptive ability such as fuzzy logic [8], swarm intelligence [9] and Max-pressure [10] have been applied to TSC.

Deep reinforcement learning(DRL) becomes very popular in adaptive traffic signal control(ATSC) due to the huge achievement and success in both reinforcement learning(RL)

and deep neural network(DNN). RL, a method where an agent learns how to act by interacting with the environment and getting feedback from the environment, has shown success in making sequential decisions and has been proved with lots of theoretical convergence properties [11]. While traditional tabular RL which stores the value of states in a table requires huge computational resources when the dimension of the state is large, DNN with function approximation has been examined successfully to approximate the value of given high-dimension input in lots of areas such as machine translation and image classification during the last few decades [12]. As a consequence, deep reinforcement learning has been examined with better generalization ability to learn in high dimension states [13]–[15].

Although early researchers have applied SARSA [16], [17] and tabular Q-learning [18] to both single intersection and multiple intersections [19]–[21] successfully, the fully centralised setting where only one agent controls all intersections costs outrageous computational resources and suffers from scalability issues and the curse of dimension in large-scale traffic networks. Since traffic signal control usually involves multiple intersections, the fully decentralised setting where one agent controls only one intersection holds better scalability and naturally leads us to consider multi-agent deep reinforcement learning(MADRL) where agents not only interact with the environment but also interact with other agents.

The simplest implementation of MRDRL is independent agents(IA). Each agent in IA only considers its own situation and maximizes its own reward and no coordination or cooperation is involved between them [22]–[24]. IA can be applied to large-scale traffic networks conveniently, but the non-stationary problem and unstable convergence property inevitably limit the performance of agents. To alleviate above issues, researchers have proposed methods to coordinate agents by either modelling optimised joint action or sharing certain information externally [25]–[29]. In [25], the max-plus algorithm is used to search the optimal joint action over agents. Tan et al. adopt iterative action search to evaluate the Q-values of different sets of joint actions [26]. Wang et al. [27] proposed a cooperative agent called Co-DQL in which the state and reward of one agent are aggregated with the average value of its neighbour agents' state, action and reward. Wei et al. [28] proposed CoLight which uses a graph attention network to embed the observations of its neighbourhood agent. As graph attention layers become deeper, the hidden layer of each agent aggregates embedded observations of all other agents. In [29], a Mess-Net is designed to embed a global state into a global message and each agent takes a part of the global message as a

RL
DRL
in
TSC
→
MARL

MADRL
in
TSC
coordination

communication

local message. Since states and Q-values are shared implicitly, agents cooperate to reach better performance.

Apart from the fully centralised setting and the fully decentralised setting, a compromised setting where each agent controls a small region of intersections has the potential to achieve scalability and hinder non-stationary meanwhile. To our best knowledge, the first paper that adopts this setting is [30]. The traffic grid network in [30] was partitioned into sub-network based on real-time situations and train agents in a centralised approximated Q-learning, while a grid traffic network is partitioned into several 2×3 sub-network and controlled in a decentralised-to-centralized manner [26] by regional DRL(R-DRL). However, in this setting, we further discuss below challenges:

- An ideal traffic network is a grid traffic network where intersections, except those on boundaries, have exactly four neighbourhoods. However, in real life, not all traffic networks are grid-like. In heterogeneous networks, it might be impossible to partition the network into desired regions. In other words, when one partition rule is forced to apply, some intersections in one region might not exist in networks. Here, we define that a region is fully-loaded if all intersections in that region exist in the network. As a result, the flexibility of partition rules is also a practical property.
- As the number of intersections in a region increases, the cardinality of action space grows exponentially. In our experiments, the simple DQN failed to converge when the cardinality of action space reaches one thousand. The search for the optimal action or less optimal actions
- The performance of a region is evaluated by all intersections in this region and how to determine the contribution of each intersection especially when the region is not fully-loaded.

To overcome the above challenges, we propose a new design of a partitioning rule and extend Branching Dueling Q-Network(BDQ) with dynamic target value computing. Experiments show that, although our agents are independent, their performance is better than some novel cooperative agents. Our main contributions are listed below.

- 1) We propose a shape-free region partition rule. The region under our partition rule include a centered intersection and its neighbourhood intersections. Subsequently, our region has no fixed shape and can be applied to heterogeneous scenarios. Due to the property of our region, in the grid traffic network, the size of a region is five and some regions are inevitably not fully-loaded. To improve convergence and generalised ability, agents are trained with centralized learning with decentralized execution(CLDE) paradigm where agents share parameters and experience buffer but execute independently.
- 2) To solve the issues that arise with not fully-loaded regions, we extend BDQ to Dynamic-BDQ(D-BDQ) in which target value and loss are computed only among activated action branches. Since each region might have different activated action branches, experiment results show that our agents under our extension have the

potential to control a dynamic number of intersections and regional traffic signal control in non-grid traffic networks.

- 3) we further examined the robustness of this partition rule by employing different partition settings. By comparing the performance of agents trained with the CLDE paradigm and decentralised training diagram, we show that our

The structure of the rest paper is arranged as follows: Section II discusses the related work of this paper. Section III introduces the background and notations of traffic signal control and MARL. Section IV formulates the and section V presents the formulation of our region agents. Section VI describes the setting of experiments and discusses the results. Section VII summarises this paper.

II. RELATED WORK

In this section, we review papers about the utilisation of information on other intersections and joint action searches in high-dimension action space. In the early stages, most researchers calculated the optimised signal plan based on strong assumptions and considering only local information. Webster [5], [6] considered one isolated intersection with uniformed traffic flow and calculates a fixed signal plan based on local information such as saturation rate and volume-to-capacity ratio. GreenWave [31] further considered the offsets between phases over neighbour intersections. Although GreenWave computes the offsets between intersections with the ratio of lane length and expected velocity, the ratio is mostly static and is hard to adapt to traffic flow that is not uniform.

In the recent decade, more researchers have realised that only local information is not enough to design intelligent controllers in a system of intersections and started to utilise information from other intersections. The most common way is to use a fully centralised agent to control all signals with the global information of one system [19]–[21]. Although this approach shows a convergence advantage in small-size traffic networks, it suffers scalability issues and poor convergence properties in large-scale traffic networks. Areal et al. [32] proposed Neighbour RL in which fully decentralised agents with linear Q-approximation controls each intersection based on a concatenation of the state of the neighbourhood intersection. To now, lots of novel algorithms based on the fully decentralised setting have been proposed to coordinate agents and share information among agents either explicitly or implicitly. Van der Pol et al. [25] modelled the traffic network as a linear combination of each intersection and apply the max-plus algorithm [33] to select joint actions. In [34], according to the congestion level between the intersection and its neighbourhoods, the agent can either choose actions by greedy algorithm or Neighbourhood Approximate Q-Learning. Tan et al. [26] proposed an iterative action search approach to search optimal joint actions. In their approach, each agent first proposes its local best action. Then, from this initial joint action search point, each agent iteratively chooses whether to deviate from its local best action based on the value computed by a global function. Although the iterative search

regional control
region challenges

main contribution

only local information

only neighbour hood information

coordination

approach offers sufficient trials for different joint actions, the effectiveness depends on the performance of the global function and the assumption that the global function is well-learned is still too strong for large-scale traffic networks.

Meanwhile, communications between intersections have been studied by lots of researchers and communications mainly bring two benefits. When designing information sharing, lots of papers have drawn their attention to the neighbourhood intersections. Varaiya [10] proposed Max-pressure in which the difference between the number of waiting vehicles of upstream intersections and downstream intersections and this idea was further applied in an MDRL framework—PressLight [35]. In CoLight [28], a Graph Attention Network is applied to compute the attention score between intersections and hidden layers are combined with their respective importance to generate graph-level attention layers. Although the observation of each agent only contain information about single agents, the hidden layer contains embedded information of all intersection as graph attention layers get deeper. Wand et al. [27] proposed Co-DQL in which the Q-values of agents converge to Nash equilibrium. In their work, the state of one intersection is concatenated with the average value of its neighbourhood intersections while the reward of one intersection is summed with a weight-average of rewards of its neighbourhood intersections. Zhang et al. [36] proposed neighbourhood cooperative hysteretic DQN(NC-HDQN) which studies the correlations between neighbourhood intersections. In their work, two methods are designed to calculate the correlation degrees of intersection. The first method named empirical NC-HDQN(ENC-HDQN) assumes that the correlation degrees of two intersections are positively related to the number of vehicles between two intersections. In ENC-HDQN, the correlation degrees are always positive and the threshold is manually defined according to the demands of traffic flows. The other method named Pearson NC-HDQN(PNC-HDQN) stores reward trajectories of each intersection and computes Pearson correlation coefficients based on those trajectories. Unlike ENC-HDQN, PNC-HDQN allows negative correlation degrees between intersections to represent the negative effects between intersections. With correlation degrees of neighbourhood intersections, the reward of one intersection is the rewards of its neighbourhood intersections multiplied with correlation degrees respectively. In ENC-HDQN, the calculation of rewards can be interpreted as a weighted average of several rewards since all coefficients are non-negative. However, in PNC-HDQN, negative coefficients might break the interpretation of the reward.

As one agent controls more intersections, the size of its action space grows exponentially. If the agent controls n intersections and each intersection offers a actions, then the cardinality of its action space is a^n . This brings problems both to sampling and convergence. To increase the efficiency of joint action searching, Lee et al. [37] proposed a weight fixing procedure and reduced the size of the output of the neural network from a^n to $a \times n$. In their method, although the size of the output of the neural network is linear, the Q-values of all actions in joint action space are still computed and the Q-values of each intersection are considered independent. Tan

implicit
com-
muni-
cation

explicit
com-
muni-
cation

detail
base-
line

joint
action
search

TABLE I
NOTION TABLE

\mathcal{V}	set of all intersections
\mathcal{E}	set of all approaches
$\text{Lane}[v]$	entering lane of intersection v
NB_{v_i}	neighbourhood intersections of v_i
$\text{wait}[l]$	number of waiting vehicles on lane l
$\text{wave}[l]$	number of vehicles on lane l
s_i	state of intersection v_i
o_i	observation of agent i

et al [26] applied a policy architecture named Wolpertinger Architecture(WA), proposed by G. Dulac-Arnold et al. [38], which searches for the optimal action based on a proto-action and applied Deep Deterministic Policy Gradient(DDPG) to perform training. In WA, the actor in DDPG generates a protocol action in continuous space. Then this protocol action is embedded and mapped to k proposed actions by the k-NN algorithm. Finally, WA chooses the action with the highest state-action value evaluated by the critic in DDPG. However, during training, DDPG computes the state-action value of the next state directly by the continuous protocol action generated by the actor. This might introduce bias during evaluating loss. The indexing of action might influence the embedding of actions and further affect policy search. Tavakol et al. proposed a new neural architecture named Branching Dueling Q-Network(BDQ) that features a shared hidden representation of state and predicts state-action value for each sub-action branching [39]. BDQ embeds the state of the agents into a shared representation. Then, the shared representation is further used to evaluate state value and compute the action advantages for each action dimension. In their architecture, the size of the outputs grows linearly and each sub-action could receive the specific loss propagation.

III. BACKGROUND

In this section, we revisit background knowledge of traffic signal control and MARL.

A. Traffic control

In a traffic network $\mathcal{G} = (\mathcal{V}, \mathcal{E})$ where $v_i \in \mathcal{V}$ represents an intersection and $e_{vu} = (v, u) \in E$ represents the approach between two intersections. The entering approach is the approach on which vehicles enter the intersection and the leaving approach is the approach on which vehicles leave the intersection. Each approach consists of a number of lanes and there are entering lanes and leaving lanes. The set of incoming lanes of intersection v_i is denoted as L_i . A traffic movement is defined as a pair of one entering lane and one leaving lane. A phase is a combination of traffic movements. As illustrated right side in figure 1, one intersection has four phases p which are North-South Straight(NS), North-South Left-turn(NSL), East-West Straight(EW) and East-West Left(EWL). A signal plan $SP = \{(p_1, t_1), (p_2, t_2), \dots\}$ is a sequence of tuples which indicates the starting time of the specific phase.

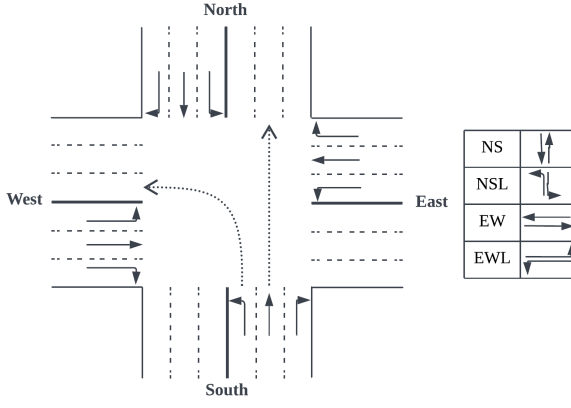


Fig. 1. Traffic network example

B. Markov Game Framework

Multi-agents system is usually modelled as a Markov Game(MG) which is defined as a tuple $\langle \mathcal{N}, \mathcal{S}, \mathcal{O}, \mathcal{A}, R, P, \gamma \rangle$ [40]. \mathcal{N} is the set of $|\mathcal{N}|$ agents. \mathcal{S} is the set of system states. $\mathcal{O} = \{\mathcal{O}_1, \dots, \mathcal{O}_{|\mathcal{N}|}\}$ is the observation space of all agents and \mathcal{O}_i of agent i is observed partially from the state of the system. $\mathcal{A} = \{\mathcal{A}_1, \dots, \mathcal{A}_{|\mathcal{N}|}\}$ is the joint action space of all agents. $r_i \in R : \mathcal{S}_i \times \mathcal{A}_1 \times \dots \times \mathcal{A}_{|\mathcal{N}|} \rightarrow \mathbb{R}$ maps a state-action pair to a real number. $P : \mathcal{S} \times \mathcal{A}_1 \times \dots \times \mathcal{A}_{|\mathcal{N}|} \times \mathcal{S} \rightarrow [0, 1]$ is the transition probability space that assigns a probability to each state-action-state transition. γ is the reward discounted factor.

The goal of MG is to find a joint optimal policy $\pi^* = \{\pi_1^*, \dots, \pi_{|\mathcal{N}|}^*\}$ under which each agent i maximizes its own expected cumulative reward

$$\mathbb{E}_{\pi_i} \left[\sum_{k=0}^{\infty} \gamma^k r_{i,t+k} | \mathcal{S}_t \right] \quad (1)$$

where $\pi_i : \mathcal{O}_i \times \mathcal{A}_i \rightarrow [0, 1]$ maps the observation of agent i to the probability distribution of its action. The action-value(Q-value) of agent i is defined as $Q_i^{\pi_i}(\mathcal{O}_i, \mathcal{A}_i) = \mathbb{E}_{\pi_i} \left[\sum_{k=0}^{\infty} \gamma^k r_{i,t+k} | \mathcal{S}_t, \pi_i(\mathcal{S}_t) \right]$. Tabular Q-learning is a classic algorithm to learn and store state-action value [18]. The update rule is formulated as

$$Q_{i,t+1}(\mathcal{O}_{i,t}, \mathcal{A}_{i,t}) = Q_{i,t}(\mathcal{O}_{i,t}, \mathcal{A}_{i,t}) + \alpha(y_t - Q_{i,t}(\mathcal{O}_{i,t}, \mathcal{A}_{i,t})) \quad (2)$$

where α is the learning rate and

$$y_t = r_{i,t} + \gamma \max_{a \in \mathcal{A}_i} Q_t(\mathcal{O}_{i,t}, a) \quad (3)$$

C. Branching Dueling Q-Network

In some complex tasks in real life such as robotic control, one task might be divided into several sub-tasks and each sub-motivation tasks contain a different number of actions. Consequently, the size of the action space grows exponentially and the credit to BDQ each sub-action becomes complex. To improve the efficiency of searching and better guide sub-actions to reach a global

goal, Travakoli et al. proposed a novel agent BDQ [39] to reduce the output size of the neural network while holding a good convergence property. Suppose an agent controls K intersection and each intersection has $|A_k|$ actions, then the cardinality of the action space of this agent is $|A_d|^k$. The size of the output of DQN grows exponentially while that of BDQ grows linearly (In Figure 2).

As illustrated in figure 2, the last shared representation layer is first used to compute common state value and then embedded to get advantage values of each action branch independently. Then the advantage values of each action branch are further aggregated with state value to calculate the Q-values of each action branch. In [39], three ways are proposed to aggregate Q-values and we select the mean advantage aggregation because it has a better stability. Formally, suppose there are K action branches and each action branch has $|A_k|$ sub-actions, The Q-value of one sub-action is calculated by the common state value and the advantage of this sub-action over the average performance of all sub-actions in this action branch. That is

$$Q_k(s, a_k) = V(s) + (A_k(s, a_k) - \frac{1}{n} \sum_{a'_k \in A_k} (A_k(s, a'_k))) \quad (4)$$

To compute the temporal difference target, we choose the mean operator as they suggested. That is

$$y = r + \gamma \frac{1}{N} \sum_d Q_d^-(s', \arg \max_{a'_d \in A_d} Q_d(s', a'_d)) \quad (5)$$

The loss function is

$$L = \mathbb{E}_{(s, a, r, s') \sim D} \left[\frac{1}{N} \sum_d (y_d - Q_d(s, a_d))^2 \right] \quad (6)$$

IV. ATSC FORMULATION

In this section, we define the formulation of state, action and reward of single intersections. In a complete episode with a length of \mathcal{T} time steps, an agent observes the environment and makes actions at every time step.

A. State Representation

There are lots of types of state representations in literature such as queue length, waiting time and delay [28], [32], [41]. In [35], vehicle wave on each lane is justified with the ability to fully describe the system while the most commonly used state representation is queue length on each lane. After careful selection among papers, we combine the one [27], [42] with the local phase. The formulation of the state of a single intersection v at time step t is defined as

$$s_v^t = \{\{wait[l]^t\}_{l \in Lane[v]}, \{wave[l]^t\}_{l \in Lane[i]}, phase^t[v]\} \quad (7)$$

B. Action space

As described above, each intersection has four phases. In TSC, two common definitions of action for one intersection are "Switch" or "Choose Phase". In the "Switch" setting, one intersection chooses whether to switch to the next predefined state reason

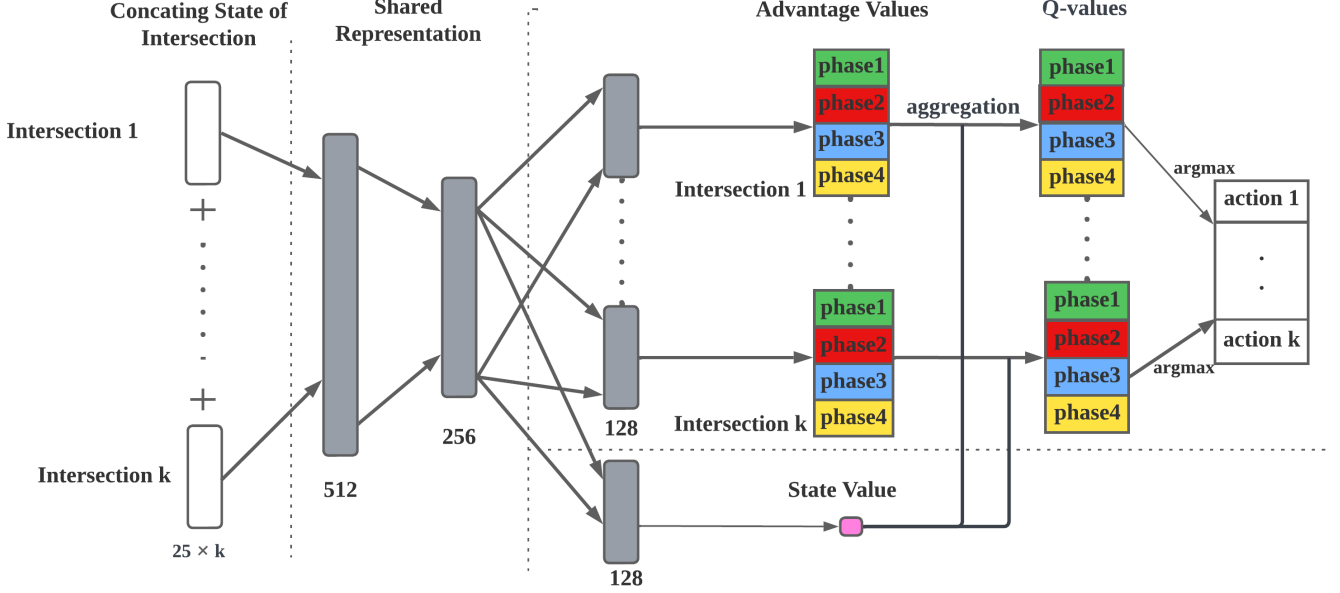


Fig. 2. Structure of BDQ. The observations of intersections are first concatenated. Then the last hidden layer of shared representation is used for both calculations of advantage values and the state value. Then, through the aggregation layer, Q-values of all action branches are calculated with advantage values and the state value based on equation 4. The size of each layer is annotated below. Hidden layers are embedded with fully connected layers and the activation is ReLu.

phase or to hold the current phase. Therefore, the `phase` states of neighbourhood intersections. In [32], the central intersection has direct access to the states of its neighbourhood intersection. In [36], the states of neighbourhood intersections are further weighted with the degree of correlation between corresponding intersections and a similar augmentation method is applied to the calculation of rewards. In [27], the states of neighbourhood intersections are averaged before augmentation. Although agents in the above works cooperate by either implicit or explicit communication, they only maximize their own rewards and non-stationary issue between agents might still limit the performance of agents. Inspired by these works, we want to utilise the best of neighbourhood intersections. In our work, an agent observes the state of all intersections in the corresponding region and tries to maximise the reward of a region of intersections.

C. Reward Design

The goal of TSC is to improve traffic conditions in a network such as reducing average travel time. However, average travel time is a delayed measurement that can be calculated only after the vehicle completes its travel. In [43], for a single intersection, using the queue length as the reward is equivalent to minimizing average travel time. In this paper, the reward of a single intersection is defined as

$$r_v^t = - \sum_{l \in Lane[v]} wait[l]^t \quad (8)$$

V. REGIONAL CONTROL AGENT IN TSC

In this section, we present our partition rules of region and MADRL training framework. Previous research has demonstrated the benefits of observing either partial or complete

phase or to hold the current phase. Therefore, the `phase` states of neighbourhood intersections. In [32], the central intersection has direct access to the states of its neighbourhood intersection. In [36], the states of neighbourhood intersections are further weighted with the degree of correlation between corresponding intersections and a similar augmentation method is applied to the calculation of rewards. In [27], the states of neighbourhood intersections are averaged before augmentation. Although agents in the above works cooperate by either implicit or explicit communication, they only maximize their own rewards and non-stationary issue between agents might still limit the performance of agents. Inspired by these works, we want to utilise the best of neighbourhood intersections. In our work, an agent observes the state of all intersections in the corresponding region and tries to maximise the reward of a region of intersections.

A. region partition rule

A region $I_v = \{v \cup NB_v\}$ centred at v is a set of intersections including v and its neighbourhood intersections. One intersection is partitioned into several regions such that $\cup_v I_v = \mathcal{V}$ and for any two regions I_v and I_v , $I_v \cap I_v = \emptyset$.

B. imaginary intersection

Our partition rule only involves the adjacency of intersections and we assume each intersection has four neighbourhood intersections. However, intersections at the boundary of grid networks have less than four neighbourhoods. As a consequence, regions under our partition rule can not cover a grid traffic network perfectly. To solve this issue, we introduce the imaginary intersection to fill the absence of neighbour

our
region
design
and
mod-
ifica-
tion

covering
issue

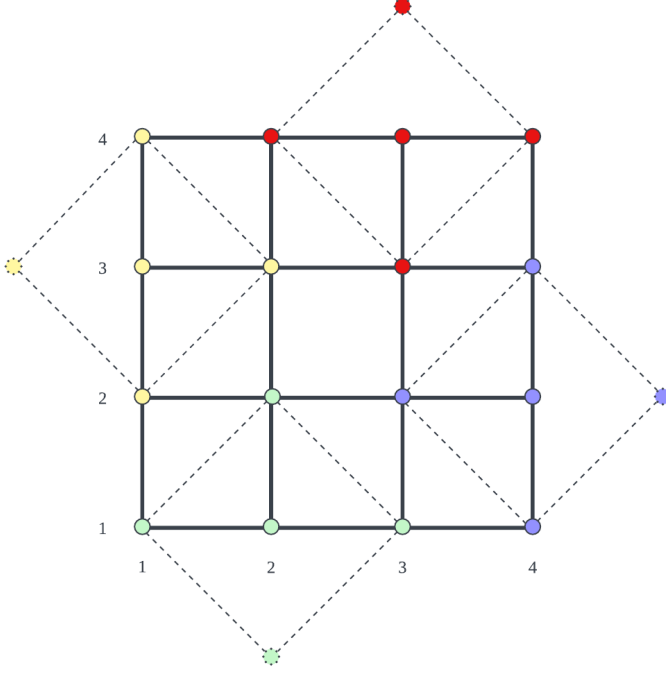


Fig. 3. A four-by-four grid network with rows and columns indexed. To best utilize all branches of BDQ, only one imaginary intersection is allowed in one region. The four-by-four grid traffic network is divided into four regions— $I_{13}, I_{21}, I_{34}, I_{42}$.

intersections. One partition example in a four-by-four grid traffic network is illustrated in figure 3.

of RL

C. RL Formulation of Regional agents

1) *Observation Representation*: An agent can observe the states of all intersections in its regions. So the observation of an agent i is a union of states of intersections. Formally,

$$O_i^t = \{s_v^t\}_{v \in I_i} \quad (9)$$

The state of an imaginary intersection is a vector of zeros.

2) *Joint Action*: Our agent controls signals of all intersections. So the joint action space of a regional agent i is

$$A_i = \{NS, NSL, EW, EWL\}^{|I_i|} \quad (10)$$

The size of the joint action space grows exponentially so does the size of the output layer in simple DQN or Actor-Critic architectures. With BDQ, the size of the output layer grows linearly. And each action branch corresponds to one particular intersection. If the corresponding intersection of one branch is not imaginary, then this action branch is activated.

3) *Reward Design*: The reward region is not studied much. Similar to [26], we assume the reward of a region is the summation of the rewards of its intersections. Regional agents tempt to minimize the waiting queue length of all intersections in the region

$$R_i^t = \sum_{v \in I_i} r_v^t \quad (11)$$

D. Dynamic-BDQ in regional signal control

BDQ was proposed to solve multi-task problems where the control is partially distributed and multi branches of actions work together such as robotic control. Similarly, we can model regional signal control as a multi-task control problem. In a region of $|I|$ intersections, there are $|I|$ action branches and each branch corresponds to one specific intersection. For agent i , the Q-value of intersection k and phase p at time step t is $Q_k(o_i^t, p)$.

Since some action branches are not activated, the original equation 5 for computing target value using an average of all branches might mislead the estimate of the target value and further deteriorate the performance of agents.

Next, we propose Dynamic-BDQ(DBDQ) in which the computation of the target values in equation 5 is further modified. Instead of calculating the average of all branches d , the Q-value of the next state is the average of activated action branches \tilde{d}

$$y_{\tilde{d}} = r + \gamma \frac{1}{\tilde{N}} \sum_{\tilde{d}} Q_{\tilde{d}}^-(s', \arg \max_{a'_{\tilde{d}} \in A_{\tilde{d}}} Q_{\tilde{d}}(s', a'_{\tilde{d}})) \quad (12)$$

Where \tilde{N} is the number of activated action branches. In the loss function, only errors of activated branches are involved

$$L = \mathbb{E}_{(s, a, r, s') \sim D} \left[\frac{1}{\tilde{N}} \sum_{\tilde{d}} (y_{\tilde{d}} - Q_{\tilde{d}}(s, a_{\tilde{d}}))^2 \right] \quad (13)$$

adaption
of
train-
ing
proce-
dure

E. Components and Pipeline of Training framework

In RL, there are two major components— Environment and agent. Agent receives observations from the environment and returns back actions. The environment then moves to the next step and passes transition tuples and the next observation to agents. The architecture of our training is illustrated in Figure 4. Since the state of the simulator needs further augmented into observation, a Pipeline class is introduced to process data from the simulator and agents. The procedure of Pipeline is listed in Algorithm 1. As shown in Figure3, the positions of imaginary intersections are different in different regions. Certain components of observations are zeros and action branches are not activated. To accelerate convergence and improve generalised ability, we adopt CLDE paradigm where agents share network parameters and experience memory.

VI. EXPERIMENTS AND RESULTS

In this section, we test our agent in both real and synthetic grid networks and compare the performance of our agent with other novel MADRL frameworks. To show the completeness and benefits of our region design, we adopt two region configurations and apply multiple combinations of region and training framework. Finally, we compare the agent CLDE paradigm.

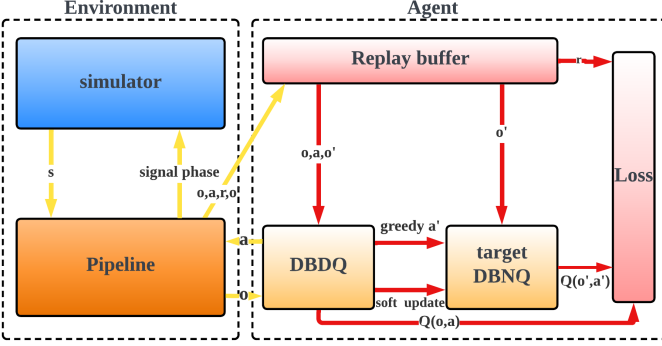


Fig. 4. The training framework of a regional agent. There are two major components—Environment and Agent. These two components communicate and exchange data through Pipeline Class. The working flow is categorized into two parts. The first part is the interaction between the agent and the environment(Yellow arrows) and the second part is the learning and updating of the agent(Red arrows). In the simulation step of the interaction part, the simulator passes the state to the pipeline and the pipeline then generates observations for agents. Based on observation, the agent chooses joint action a under ϵ -greedy policy and passes the joint action to the pipeline. Finally, the pipeline passes signal phases to simulation and moves to the next simulation step.

Algorithm 1 Algorithm for Pipeline

```

1: Initialise DBDQ  $\theta_i$  and target DBDQ  $\theta_i^- \leftarrow \theta_i$ 
2: Initialise Replay Memory  $M_i$ , Region Configuration  $I$ 
3: while  $i < episode$  do
4:    $s \leftarrow$  environment reset
5:    $o_i \leftarrow$  generate observation based on  $s, I$ 
6:   while  $t < T$  do
7:     if  $rand < \epsilon$  then
8:        $a_i \leftarrow$  random joint action
9:     else
10:       $a_i \leftarrow \cup_{\tilde{d}} \arg \max_{a'_{\tilde{d}}} Q_{\tilde{d}}(o_i, a'_{\tilde{d}})$ 
11:    end if
12:     $r, s' \leftarrow$  env step after all agents choose actions
13:    calculate  $R_i$  and generate  $o'_i$  based on  $s', I$ 
14:    store transition  $(o_i, a, R_i, o'_i)$  to  $M_i$ 
15:    Update  $\theta$  by Eq. 6 with target value by Eq. 12
16:     $\theta^- \leftarrow (1 - \tau)\theta^- + \tau\theta$  for certain step
17:     $o_i \leftarrow o'_i$ 
18:  end while
19: end while

```

A. Experiment Scenario

The traffic simulator CityFlow we used in this paper is an open-source simulator [44]. In our experiment, two four-by-four grid networks—one real(Hangzhou) and one synthetic are used. Their major difference is the length of approaches. The distance between two adjacent intersections in the Hangzhou network is 800m and that in the synthetic network is 300m. In the Hangzhou network, two traffic flows are applied—one is in flat hours and the other is in peak hours. The data is based on the camera data in Hangzhou and is further simplified. In the synthetic network, the flow is generated according to Gaussian distribution. The turning ratio for all flow is distributed as 10%(left turn), 60%(straight) and 30%(right

TABLE II
FLOW STATISTICS

Flow	Arrival Rate(vehicles/s)	
	Mean	Std
(Hangzhou) Flat	0.83	1.33
(Hangzhou) Peak	1.82	2.15
Synthetic	3.12	4.08

TABLE III
HYPERPARAMETER SUMMARY

Component	Hyperparameter	Value
DBDQ	γ	0.99
	Learning rate α	0.0001
	Replay Buffer Size	200000
	Network optimizer	Adam
	Activation Function	Relu
	τ	0.001
R-DRL	Batch Size	32
	k	128
	α_{critic}	0.0001
ϵ -greedy Policy	α_{actor}	0.00001
	ϵ_{\max}	1
	ϵ_{\min}	0.001
	decay steps	20000

turn). The summarised statistics are listed in table II. In the table, the arrival rate of synthetic flow is the highest and both flat flow and peak flow in the real network can test the performance of RL agents in the real world. All these datasets are open-sourced¹.

The overall time span for all flows is 3600s and some vehicles arrive near the end of the time span. To obtain a complete performance, we set the simulator to simulate 4000s to allow more vehicles to arrive at their destinations. To avoid signals flicking too frequently, all agents perform actions for every $\Delta t = 10$ s and no yellow phase is inserted between different phases. Then the length T of one episode is 400.

We compare our agent with the following baselines—Fixed time, NeighbourRL, R-DRL, CoLight², PNC-HDQN and ENC-HDQN³. For DBDQ, the network structure follows the original paper [39] and is demonstrated in Figure 2. The size of hidden layers of NeighbourRL is the same as DBDQ. For R-DRL, the structures of actor and critic follow the description in [26]. Although a global critic is proposed to coordinate R-DRL, the convergence of this global critic is not guaranteed. So only independent R-DRL is compared. The hyperparameters for our agent, NeighbourRL and R-DRL are listed in table III. For other baselines, we run the source code for fairness.

B. Metric

Similarly to [36], we choose below three metrics to evaluate the performance of agents.

- Average Travel Time(ATT): average of all vehicles' travel time. Since the time step of our simulation is large than the arrival time span, all vehicles can travel in the network for enough time and the computation of ATT is more

¹<https://traffic-signal-control.github.io/#open-datasets>

²<https://github.com/wingsweihua/colight>

³<https://github.com/RL-DLMU/PNC-HDQN>

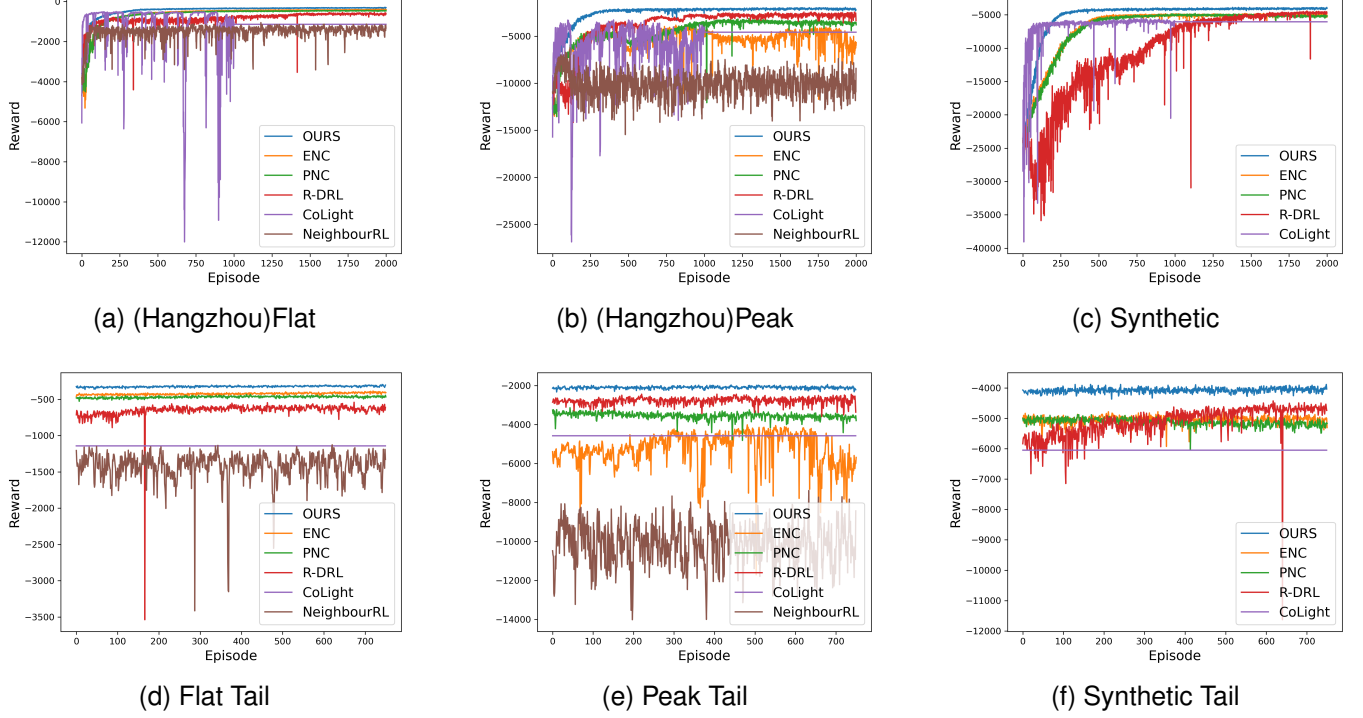


Fig. 5. Learning curve of RL agents. Top three pictures are overall performance during 2000 episodes and bottom three pictures are overall performance after episode 1250

TABLE IV
NUMERICAL STATISTICS

Flow	Metric	Fixed	NeighbourRL	R-DRL	CoLight	PNC	ENC	OURS
Flat	ATT	482.19	379.83 ± 8.37	335.29 ± 1.65	334.01 ± 0.95	328.13 ± 0.49	326.23 ± 0.59	319.14 ± 0.43
	AQL	0.57	0.29 ± 0.031	0.13 ± 0.01	0.28 ± 0.34	0.10 ± 0.0020	0.09 ± 0.0021	0.07 ± 0.0016
	TP	2810	2930.79 ± 7.19	2950.75 ± 3.81	2899.92 ± 144.7	2942.9 ± 3.09	2959.776 ± 1.60	2963.27 ± 0.89
Peak	ATT	803.78	675.01 ± 60.26	415.75 ± 4.94	463.7 ± 7.11	437.09 ± 5.84	479.25 ± 26.14	402.02 ± 3.00
	AQL	1.8	2.17 ± 0.21	0.58 ± 0.04	1.31 ± 0.37	0.75 ± 0.03	1.12 ± 0.23	0.44 ± 0.01
	TP	5105	5669.4 ± 226.92	6340.18 ± 18.28	6034 ± 370.6	6296.85 ± 29.96	6222.2 ± 136.89	6382.19 ± 10.9
Synthetic	ATT	548.77	-	216.03 ± 7.28	246.14 ± 18.19	228.24 ± 2.0	224.6 ± 1.6	206.6 ± 1.3
	AQL	3.32	-	0.99 ± 0.1	1.27 ± 0.2	1.08 ± 0.02	1.05 ± 0.02	0.85 ± 0.016
	TP	9553	-	11173.29 ± 63.63	11179.2 ± 201.3	11179.8 ± 15.67	11215.41 ± 4.96	11227.93 ± 1.07

complete and less affected by vehicles which just start their trip

- Average Queue Length(AQL): average queue length on each lane of all intersection. The definition of the reward of our agent is the sum of queue length. So AQL is a direct numerical interpretation of reward.
- Throughput(TP): number of vehicles which arrive at the destination. While reducing ATT, we also want to increase throughput so that benefits are maximized

C. Overall performance

In Figure 5, the reward curves of all RL agents are plotted. Since the definitions of the reward of other baselines involve augmentations, we computed the episode reward as the below equation for consistency.

$$R = \frac{1}{|\mathcal{V}|} \sum_{t=1}^{\mathcal{T}} \sum_v r_v^t \quad (14)$$

As illustrated in Figure 5, our agent converged in all three scenarios and the convergence speed was faster than other RL agents except CoLight. The converge speed of CoLight was the fastest because it adopted the Monte Carlo training method. NeighbourRL failed to converge in the synthetic scenarios and the corresponding curves and numerical data were omitted. From the bottom figures in Figure 5, our agent achieved the highest reward after convergence. As the volume of vehicles increases, the curves started to oscillate and the curve in synthetic is the most unstable. However, our agent was the most stable one and with the smallest fluctuation. Numerical results are listed in Table IV. In the Hangzhou scenario, as the flow density increases, the average travel time becomes larger and the network become crowded. It is interesting that R-DRL performed better during peak hours than other baselines. This is likely because the observation of agents in the flat hour is a sparse vector while that in peak hour contains more complete information on traffic dynamics. In the synthetic scenario, the average travel time of vehicles is

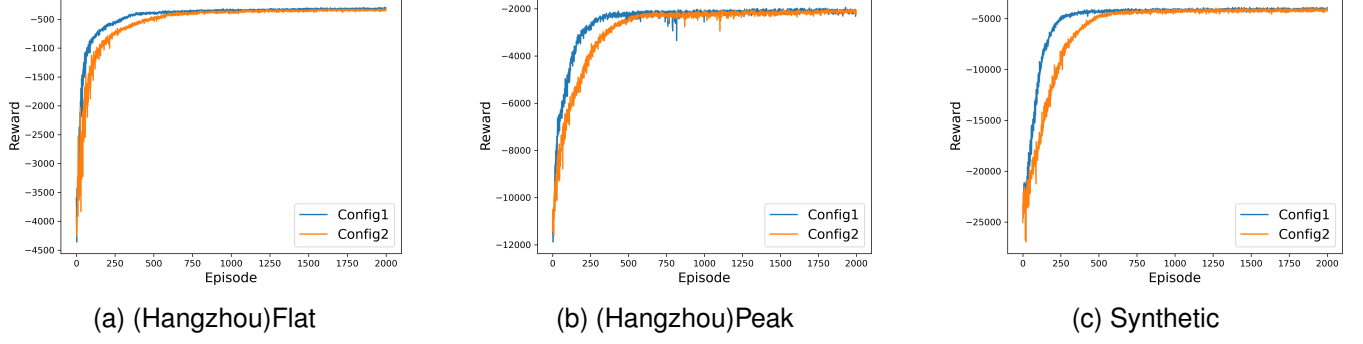


Fig. 6. Learning curve of two configurations.

the shortest and the average queue length is highest because the intersections in the synthetic network are much closer than those in the Hangzhou network. Although the arrival rate of the synthetic scenario is highest, the average queue length of regional agents almost doubled that in Hangzhou peak hour while those of other baselines. This is probably caused by the distance between intersections. If intersections are distant, the travel time between intersections becomes longer and agents have more chance to find a better policy. The difference in throughput between agents is not significant because simulation steps are large enough for most vehicles to arrive at their destinations. Overall, our agent achieved the best results and standard deviation among all metrics.

D. Robustness of our region

As illustrated in Figure 3, we balanced the number of activated branches as much as we can. There are two configurations of regions—one is $I_{13}, I_{21}, I_{34}, I_{42}$ as it is shown in Figure 3 and the other configuration is $I_{12}, I_{24}, I_{31}, I_{43}$. To ensure the completeness of the experiment, we compare the performance of agents under both configurations and the learning curves are plotted in Figure 6. Agents under both configurations converge but Config2 has a slower convergence speed in all scenarios. These training curves indicate that the configuration of regions can affect the training process of agents. In different configurations, agents observe different sets of intersections and traffic flows of these intersections are different. The intersections of regions in configuration 1 might share higher correlations. In Table V, although the numerical results of configuration 1 are better than those of configuration 2, there is no significant difference and the numerical results of configuration 2 are better than the results of other baselines.

E. improvement of DBDQ

The target value of DBDQ only involves activated branches to remove the influence of imaginary intersections. To show the advantage of DBDQ, we combined BDQ with "Config1" and DBDQ with a 2-by-3 grid region in R-DRL. "Config1" has one imaginary intersection and the grid region has two imaginary intersections. Both regions have four activated branches in BDQ and DBDQ. In table VI, the performance of both

TABLE V
NUMERICAL STATISTICS OF TWO CONFIGURATIONS

Flow	Metric	Config1	Config2
Flat	ATT	319.14 \pm 0.43	320.62 \pm 0.48
	AQL	0.07 \pm 0.0016	0.07 \pm 0.0019
	TP	2963.27 \pm 0.89	2963.03 \pm 0.81
Peak	ATT	402.02 \pm 3.00	406.99 \pm 4.67
	AQL	0.438 \pm 0.01	0.443 \pm 0.009
	TP	6382.19 \pm 10.9	6369.724 \pm 15.2
Synthetic	ATT	206.6 \pm 1.3	208.27 \pm 1.27
	AQL	0.85 \pm 0.0157	0.86 \pm 0.0162
	TP	11227.93 \pm 1.07	11227.41 \pm 1.34

TABLE VI
IMPROVEMENT BY DBDQ

Flow	Metric	config1	grid
Flat	ATT	2.8%	3.5%
	AQL	9.7%	24.1%
	TP	0.14%	0.27%
Peak	ATT	1.1%	1.8%
	AQL	7.8%	19.3%
	TP	0.12%	0.42%
Synthetic	ATT	1.7%	2.4 %
	AQL	8.5%	11.8%
	TP	0.27%	0.34%

region configurations is improved by DBDQ. For different scenarios, the improvement in the Hangzhou flat scenario is more significant than that in other scenarios. It is likely that . For different region configurations, the improvement of the grid region is more significant than config1. It is very likely that there are more imaginary intersections in grid regions and DBDQ can estimate a less biased target value.

VII. CONCLUSION AND FUTURE WORK

In this paper, we proposed a new regional control agent for ATSC in which the region is partitioned by the adjacency of intersections. Meanwhile, we applied DBDQ to search for joint action and to release the negative influence of imaginary intersections. Our region design has the potential to be applied in heterogeneous networks. There are two major advantages of DBDQ. One is that the size of joint action space grows linearly as the number of intersections in the region increase so the search for optimal actions is more efficient. The other is that DBDQ alleviates the influence of imaginary intersections by calculating target values based on activated branches.

We have carried out thorough experiments to evaluate the performance and robustness of our agent. Experiments show that our agent achieves the best performance in both real and synthetic scenarios, especially in scenarios with a high-density flow. Also, we observed that the distance between intersections can limit more or less the learning of agents and their potential. It is interesting that, although the performance of different configurations is very similar, a different configuration can influence the convergence of agents.

REFERENCES

- [1] “Inrix 2021 global traffic scorecard: As lockdowns ease uk city centres show signs of return to 2019 levels of congestion,” 2022. [Online]. Available: <https://inrix.com/press-releases/2021-traffic-scorecard-uk/>
- [2] “Inrix: Americans lost 3.4 billion hours due to congestion in 2021, 42% below pre-covid,” 2022. [Online]. Available: <https://inrix.com/press-releases/2021-traffic-scorecard-uk/>
- [3] “smog, soot, and other air pollution from transportation,” 2022. [Online]. Available: <https://www.epa.gov/transportation-air-pollution-and-climate-change/smog-soot-and-other-air-pollution-transportation>
- [4] “who releases country estimates on air pollution exposure and health impact_2022,” 2022. [Online]. Available: [www.who.int/news-item/27-09-2016-who-releases-country-estimates-on-air-pollution-exposure-and-health-impact_2022](http://www.who.int/news-room/27-09-2016-who-releases-country-estimates-on-air-pollution-exposure-and-health-impact_2022)
- [5] F. V. Webster, “Traffic signal settings,” Tech. Rep., 1958.
- [6] P. Koonce and L. Rodegerdts, “Traffic signal timing manual.” United States. Federal Highway Administration, Tech. Rep., 2008.
- [7] J. D. Little, M. D. Kelson, and N. H. Gartner, “Maxband: A versatile program for setting signals on arteries and triangular networks,” 1981.
- [8] M. B. Trabia, M. S. Kaseko, and M. Ande, “A two-stage fuzzy logic controller for traffic signals,” *Transportation Research Part C: Emerging Technologies*, vol. 7, no. 6, pp. 353–367, 1999.
- [9] H. Ceylan and M. G. Bell, “Traffic signal timing optimisation based on genetic algorithm approach, including drivers’ routing,” *Transportation Research Part B: Methodological*, vol. 38, no. 4, pp. 329–342, 2004.
- [10] P. Varaiya, “Max pressure control of a network of signalized intersections,” *Transportation Research Part C: Emerging Technologies*, vol. 36, pp. 177–195, 2013.
- [11] R. S. Sutton and A. G. Barto, *Reinforcement learning: An introduction*. MIT press, 2018.
- [12] Y. LeCun, Y. Bengio, and G. Hinton, “Deep learning,” *nature*, vol. 521, no. 7553, pp. 436–444, 2015.
- [13] V. Mnih, K. Kavukcuoglu, D. Silver, A. A. Rusu, J. Veness, M. G. Bellemare, A. Graves, M. Riedmiller, A. K. Fidjeland, G. Ostrovski *et al.*, “Human-level control through deep reinforcement learning,” *nature*, vol. 518, no. 7540, pp. 529–533, 2015.
- [14] J. Kober, J. A. Bagnell, and J. Peters, “Reinforcement learning in robotics: A survey,” *The International Journal of Robotics Research*, vol. 32, no. 11, pp. 1238–1274, 2013.
- [15] O. Vinyals, I. Babuschkin, J. Chung, M. Mathieu, M. Jaderberg, W. M. Czarnecki, A. Dudzik, A. Huang, P. Georgiev, R. Powell *et al.*, “AlphaStar: Mastering the real-time strategy game starcraft ii,” *DeepMind blog*, vol. 2, 2019.
- [16] G. A. Rummery and M. Niranjan, *On-line Q-learning using connectionist systems*. Citeseer, 1994, vol. 37.
- [17] R. S. Sutton, “Generalization in reinforcement learning: Successful examples using sparse coarse coding,” *Advances in neural information processing systems*, vol. 8, 1995.
- [18] C. J. Watkins and P. Dayan, “Q-learning,” *Machine learning*, vol. 8, no. 3, pp. 279–292, 1992.
- [19] T. L. Thorpe and C. W. Anderson, “Traffic light control using sarsa with three state representations,” *Technical report, Citeseer*, 1996.
- [20] K. Wen, S. Qu, and Y. Zhang, “A stochastic adaptive control model for isolated intersections,” in *2007 IEEE International Conference on Robotics and Biomimetics (ROBIO)*. IEEE, 2007, pp. 2256–2260.
- [21] S. El-Tantawy and B. Abdulhai, “An agent-based learning towards decentralized and coordinated traffic signal control,” in *13th International IEEE Conference on Intelligent Transportation Systems*. IEEE, 2010, pp. 665–670.
- [22] J. Ault, J. P. Hanna, and G. Sharon, “Learning an interpretable traffic signal control policy,” in *AAMAS*, 2020.
- [23] J. A. Calvo and I. Dusparic, “Heterogeneous multi-agent deep reinforcement learning for traffic lights control.” in *AICS*, 2018, pp. 2–13.
- [24] M. Abdoos, N. Mozayani, and A. L. Bazzan, “Traffic light control in non-stationary environments based on multi agent q-learning,” in *2011 14th International IEEE conference on intelligent transportation systems (ITSC)*. IEEE, 2011, pp. 1580–1585.
- [25] E. Van der Pol and F. A. Oliehoek, “Coordinated deep reinforcement learners for traffic light control,” *Proceedings of learning, inference and control of multi-agent systems (at NIPS 2016)*, vol. 1, 2016.
- [26] T. Tan, F. Bao, Y. Deng, A. Jin, Q. Dai, and J. Wang, “Cooperative deep reinforcement learning for large-scale traffic grid signal control,” *IEEE transactions on cybernetics*, vol. 50, no. 6, pp. 2687–2700, 2019.
- [27] X. Wang, L. Ke, Z. Qiao, and X. Chai, “Large-scale traffic signal control using a novel multiagent reinforcement learning,” *IEEE transactions on cybernetics*, vol. 51, no. 1, pp. 174–187, 2020.
- [28] H. Wei, N. Xu, H. Zhang, G. Zheng, X. Zang, C. Chen, W. Zhang, Y. Zhu, K. Xu, and Z. Li, “Colight: Learning network-level cooperation for traffic signal control,” in *Proceedings of the 28th ACM International Conference on Information and Knowledge Management*, 2019, pp. 1913–1922.
- [29] D. Xie, Z. Wang, C. Chen, and D. Dong, “Iedqn: Information exchange dqn with a centralized coordinator for traffic signal control,” in *2020 International Joint Conference on Neural Networks (IJCNN)*. IEEE, 2020, pp. 1–8.
- [30] T. Chu, S. Qu, and J. Wang, “Large-scale traffic grid signal control with regional reinforcement learning,” in *2016 american control conference (acc)*. IEEE, 2016, pp. 815–820.
- [31] R. P. Roess, E. S. Prassas, and W. R. McShane, *Traffic engineering*. Pearson/Prentice Hall, 2004.
- [32] C. Liu, T. Urbanik, and A. G. Kohls, “Reinforcement learning-based multi-agent system for network traffic signal control,” *IET Intelligent Transport Systems*, vol. 4, no. 2, pp. 128–135, 2010.
- [33] J. R. Kok and N. Vlassis, “Using the max-plus algorithm for multiagent decision making in coordination graphs,” in *Robot Soccer World Cup*. Springer, 2005, pp. 1–12.
- [34] T. Tan, T. Chu, B. Peng, and J. Wang, “Large-scale traffic grid signal control using decentralized fuzzy reinforcement learning,” in *Proceedings of SAI Intelligent Systems Conference (IntelliSys) 2016: Volume 1*. Springer, 2018, pp. 652–662.
- [35] H. Wei, C. Chen, G. Zheng, K. Wu, V. Gayah, K. Xu, and Z. Li, “Presslight: Learning max pressure control to coordinate traffic signals in arterial network,” in *Proceedings of the 25th ACM SIGKDD International Conference on Knowledge Discovery & Data Mining*, 2019, pp. 1290–1298.
- [36] C. Zhang, Y. Tian, Z. Zhang, W. Xue, X. Xie, T. Yang, X. Ge, and R. Chen, “Neighborhood cooperative multiagent reinforcement learning for adaptive traffic signal control in epidemic regions,” *IEEE Transactions on Intelligent Transportation Systems*, vol. 23, no. 12, pp. 25157–25168, 2022.
- [37] J. Lee, J. Chung, and K. Sohn, “Reinforcement learning for joint control of traffic signals in a transportation network,” *IEEE Transactions on Vehicular Technology*, vol. 69, no. 2, pp. 1375–1387, 2019.
- [38] G. Dulac-Arnold, R. Evans, H. van Hasselt, P. Sunehag, T. Lillicrap, J. Hunt, T. Mann, T. Weber, T. Degrif, and B. Coppin, “Deep reinforcement learning in large discrete action spaces,” *arXiv preprint arXiv:1512.07679*, 2015.
- [39] A. Tavakoli, F. Pardo, and P. Kormushev, “Action branching architectures for deep reinforcement learning,” in *Proceedings of the aaai conference on artificial intelligence*, vol. 32, no. 1, 2018.
- [40] M. L. Littman, “Markov games as a framework for multi-agent reinforcement learning,” in *Machine learning proceedings 1994*. Elsevier, 1994, pp. 157–163.
- [41] H. Wei, G. Zheng, H. Yao, and Z. Li, “Intellilight: A reinforcement learning approach for intelligent traffic light control,” in *Proceedings of the 24th ACM SIGKDD International Conference on Knowledge Discovery & Data Mining*, 2018, pp. 2496–2505.
- [42] T. Chu, J. Wang, L. Codeca, and Z. Li, “Multi-agent deep reinforcement learning for large-scale traffic signal control,” *IEEE Transactions on Intelligent Transportation Systems*, vol. 21, no. 3, pp. 1086–1095, 2019.
- [43] G. Zheng, X. Zang, N. Xu, H. Wei, Z. Yu, V. Gayah, K. Xu, and Z. Li, “Diagnosing reinforcement learning for traffic signal control,” *arXiv preprint arXiv:1905.04716*, 2019.
- [44] H. Zhang, S. Feng, C. Liu, Y. Ding, Y. Zhu, Z. Zhou, W. Zhang, Y. Yu, H. Jin, and Z. Li, “Cityflow: A multi-agent reinforcement learning environment for large scale city traffic scenario,” in *The world wide web conference*, 2019, pp. 3620–3624.